Res Chem Intermed
DOI 10.1007/s11164-012-0959-1

Pd nanoparticles immobilized on boehmite by using tannic acid as structure-directing agent and stabilizer: a high performance catalyst for hydrogenation of olefins

Jing Liu · Xuepin Liao · Bi Shi

Received: 6 October 2012 / Accepted: 27 November 2012

Abstract Boehmite-supported Pd nanoparticles (Pd–TA–boehmite) were successfully synthesized by a hydrothermal method using tannic acid as the structure-directing agent as well as stabilizer. The physicochemical properties of the Pd–TA–boehmite catalyst were well characterized by XPS, XRD, N_2 adsorption/desorption, and TEM analyses. Catalytic hydrogenation of olefins was used as the probe reaction to evaluate the activity of the Pd–TA–boehmite catalyst. For comparison, the Pd–boehmite catalyst prepared without tannic acid was also employed for olefin hydrogenation. For all the investigated substrates, the Pd–TA–boehmite catalyst exhibited superior catalytic performance than the Pd–boehmite catalyst. For the example of hydrogenation of allyl alcohol, the initial hydrogenation rate and selectivity of the Pd–TA–boehmite catalyst were 23,520 mol/mol h and 99 %, respectively, while those of the Pd–boehmite catalyst were only 14,186 mol/mol h and 93 %, respectively. Additionally, the hydrogenation rate of the Pd–TA–boehmite catalyst could still reach 20,791 mol/mol h at the 7th cycle, which was much higher than that of the Pd–boehmite catalyst (5,250 mol/mol h) at the 4th cycle, thus showing an improved reusability.

Keywords Pd nanoparticle · Boehmite · Tannic acid · Hydrogenation · Catalytic activity · Reusability

J. Liu · X. Liao (✉)
Department of Biomass Chemistry and Engineering, Sichuan University, Chengdu 610065, People's Republic of China
e-mail: xpliao@scu.edu.cn

B. Shi
National Engineering Laboratory for Clean Technology of Leather Manufacture, Sichuan University, Chengdu 610065, People's Republic of China

Published online: 12 December 2012

Introduction

Metal nanoparticle catalysts show very high catalytic activity in a variety of chemical reactions because of their high surface-to-volume ratio, high surface energy and large surface curvature [1–3]. In general, metal nanoparticle catalysts are prepared by immobilizing metal nanoparticles onto inorganic solid matrices [4, 5]. However, the as-prepared heterogeneous catalysts often suffer the problems of aggregation and leaching-out of active species due to their high surface energy and weak interaction with the matrices, which inevitably lead to reduced catalytic activity and reusability [6, 7], and great efforts have been made to solve these problems. One frequently used strategy is to encapsulate metal nanoparticles into porous supports [8, 9], whereas their preparation processes often involve the unfavorable high temperature calcination of inorganic supports. Another possible method is to functionalize the supports with specific organic molecular ligands or surfactant to stabilize metal nanoparticles [10, 11], but the relatively high cost and/or complicated procedures make these approaches less attractive for industrial applications. Thus, it remains highly desirable to find new approaches to prepare heterogeneous metal nanoparticle catalysts with high activity and stability.

Recently, natural macromolecules as environment-friendly stabilizers have attracted growing attention for metal nanoparticle synthesis due to their special physicochemical properties. For instance, cellulose rich in ether oxygen and hydroxyl groups can stabilize metal nanoparticles (Ag, Au, Pt, Pd) [12, 13]. Silk fibroin with abundant thiol and amine groups is able to in situ reduce Au^{3+} ions to Au nanoparticles and further stabilize them in a highly monodispersed nature [14]. Among them, plant tannin, a kind of natural biomass widely distributed in plant leaf and fruit, has been found to have the ability to chelate with many metal ions by the formation of a five-membered chelated ring and further stabilize the corresponding metal nanoparticles [15, 16]. Accordingly, it can be reasoned that plant tannins can act as the stabilizer to immobilize metal nanoparticles on the supporting matrices.

Boehmite, a commonly used supporting matrix, is usually prepared by a hydrothermal method [17]. Previous researches have shown that the addition of specific polymers and/or surfactants can direct the crystal growth and morphology of boehmite during the hydrothermal process [18, 19]. Considering that tannic acid possesses some surfactant-like characteristics [20], it is possible to direct the crystal growth of boehmite by using tannic acid as the additive. During the hydrothermal process, tannic acid will chelate with aluminum in the boehmite lattice through its dense ortho-phenolic hydroxyls, and influence the structural properties of boehmite, such as specific surface area and pore size. Moreover, the residual adjacent phenolic hydroxyls of tannic acid may also chelate with Pd^{2+}, and further stabilize the corresponding Pd nanoparticles generated after reduction. As a consequence, tannic acid can act as bridge to link metal nanoparticles and boehmite with strong interaction, which will ensure even distribution and high stability of the Pd nanoparticles on boehmite. Based on the above strategy, a novel method for the synthesis of boehmite immobilized Pd nanoparticles (Pd–TA–boehmite) was developed in this work. The influence of introducing tannic acid on the distribution of Pd nanoparticles and the crystal structure of the boehmite were investigated.

The catalytic activity and stability of the Pd–TA–boehmite catalyst were evaluated by using hydrogenation of olefins as the probe reaction.

Experimental

Reagents

Palladium chloride ($PdCl_2$), $Al(NO_3)_3{\cdot}9H_2O$, tannic acid, allyl alcohol, a-methacrylic acid, styrene, methanol and other chemicals were all analytic reagents and used without further purification.

Preparation of the Pd–TA–boehmite catalyst

30 mL of 0.8 mol/L $Al(NO_3)_3{\cdot}9H_2O$ solution was slowly dropped into 50 mL of tannic acid solution (3.5 wt%) under stirring. The pH of the mixture was adjusted to 4.5 using ammonia aqueous solution (5 wt%) and kept stirring for 1 h. The resultant suspension was sealed in a Teflon-lined stainless steel autoclave and maintained at 160 °C for 48 h under N_2 atmosphere. After cooling naturally to room temperature, the precipitate was centrifuged, washed with distilled water, and dried at 60 °C for 24 h. The obtained intermediate product was denoted as TA–boehmite.

Next, 1.0 g of the obtained TA–boehmite was mixed with 10 mL of 1.0 g/L Pd^{2+} solution under stirring for 24 h, and the Pd^{2+} absorbed on TA–boehmite (Pd^{2+}–TA–boehmite) was further reduced by $NaBH_4$ solution. The resultant Pd–TA–boehmite was centrifuged, washed with distilled water, and dried under vacuum at 60 °C for 24 h. For comparison, Pd–boehmite was prepared using a similar method but without the use of tannic acid.

Characterization

X-ray photoelectron spectroscopy (XPS, Kratos XSAM-800, UK) analysis was conducted by employing Mg-Kα X radiation ($hv = 1{,}253.6$ eV) and a pass energy was 31.5 eV. All of the binding energy peaks of XPS spectra were calibrated by placing the principal C 1 s binding energy peak at 284.7 eV. The crystalline structures were characterized by XRD (X'Pert Pro, Philips PW3040/60, Netherlands) with Cu-Kα radiation. The specific surface area and pore structure of catalysts were analyzed by N_2 adsorption/desorption using surface area and porosity analyzer (BET, Micromeritics Tristar 3000, USA). Transmission electron microscopy (TEM; Jeol 2010, Japan) performed at an acceleration voltage of 200 kV was used to observe the morphology of the Pd nanoparticles in the catalysts. The compositions of the catalytic reaction system were analyzed by gas chromatography (Shimadzu, CG-2010, China).

Catalytic hydrogenation of olefins

A specific amount of catalyst (containing 2.5 μmol Pd) and catalytic substrate (10 mmol) were added to 20 mL of methanol in the autoclave. Then, the autoclave

was heated to 30 °C under constant stirring (1,200 rpm) and 1 MPa H_2 atmosphere. When the reaction was completed, the products were analyzed by gas chromatograph and the catalyst was recovered for reuse. The activity of the catalyst was evaluated by the initial hydrogenation rate (mol/Pd mol h) determined by the initial slope of the curve of product yield versus time [21].

Results and discussion

Preparation mechanism of Pd–TA–boehmite

The XPS analyses supply the opportunity to understand the preparation mechanism of the Pd–TA–boehmite catalyst. As shown in Fig. 1A, the O 1s peak of TA–boehmite can be fitted into three contributions. Two major peaks are located at 531.56 and 532.60 eV, respectively, which are correspondingly correlated to boehmite [22] and phenolic hydroxyl of tannic acid [23]. A small peak located at 533.15 eV is the up-shift of phenolic hydroxyl, and can be assigned to phenolic oxygen chelated with metal ions [23, 24]. These results confirm that the chelation reaction between Al^{3+} ions and tannic acids took place during the hydrothermal process, and therefore tannic acid was successfully in situ immobilized on boehmite.

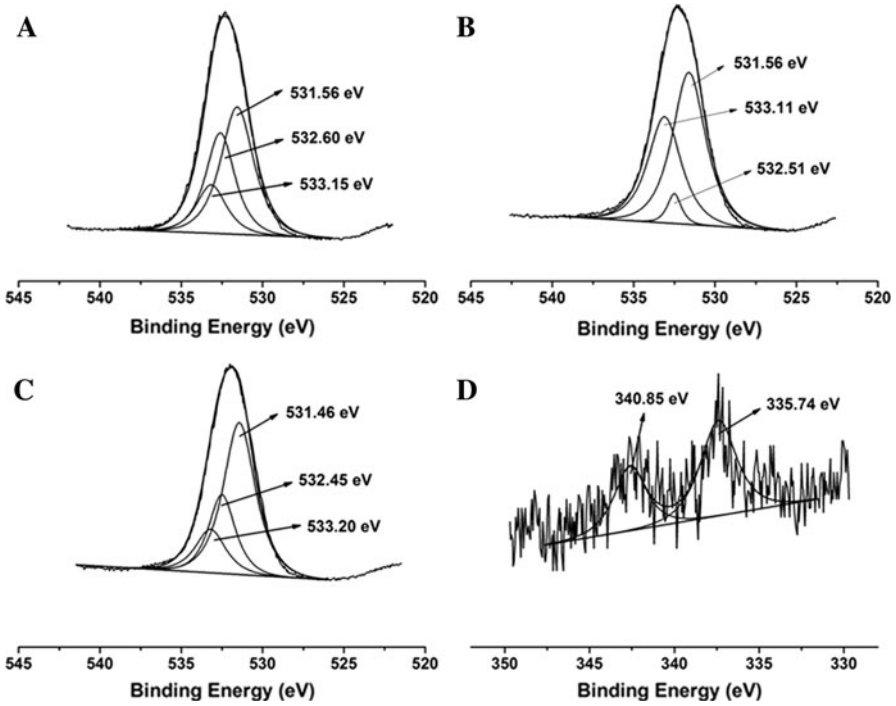

Fig. 1 O1s XPS spectrum of TA–boehmite (**A**), Pd^{2+}–TA–boehmite (**B**) and Pd–TA–boehmite (**C**); Pd 3d XPS spectrum of Pd–TA–boehmite (**D**)

After the adsorption of TA–boehmite to Pd^{2+} ions, the peak intensity at 532.51 eV assigned to phenolic hydroxyl obviously decreases in comparison with that of TA–boehmite (532.60 eV, Fig. 1A), while the peak intensity at 533.11 eV related to chelated phenolic oxygen sharply increases compared with that of TA–boehmite (533.15 eV; Fig. 1A). These observations indicate that Pd^{2+} ions were chelated by the phenolic hydroxyls of TA–boehmite and therefore more chelated phenolic oxygen was generated in Pd^{2+}–TA–boehmite.

In contrast, in the O 1s spectrum of the final product of Pd–TA–boehmite (Fig. 1C), the peak intensity at 532.45 eV of phenolic hydroxyl becomes intense along with the peak intensity at 533.20 eV of chelated phenolic oxygen being weak. In addition, the Pd 3d spectrum of Pd–TA–boehmite (Fig. 1D) has two characteristic peaks of element Pd(0), 340.85 and 335.74 eV [25]. These observations suggest that, during the process of Pd^{2+} reduction, a part of the chelated phenolic hydroxyls was released and converted into phenolic hydroxyls via recombining with protons from $NaBH_4$. Meanwhile, the intensity ratio of chelated phenolic oxygen to phenolic oxygen is higher in Pd–TA–boehmite than that in TA–boehmite, which indicates that the generated Pd(0) nanoparticles were still anchored by the phenolic hydroxyls of tannic acid. On the basis of the above analyses, the synthetic route of Pd–TA–boehmite can be deduced as Fig. 2.

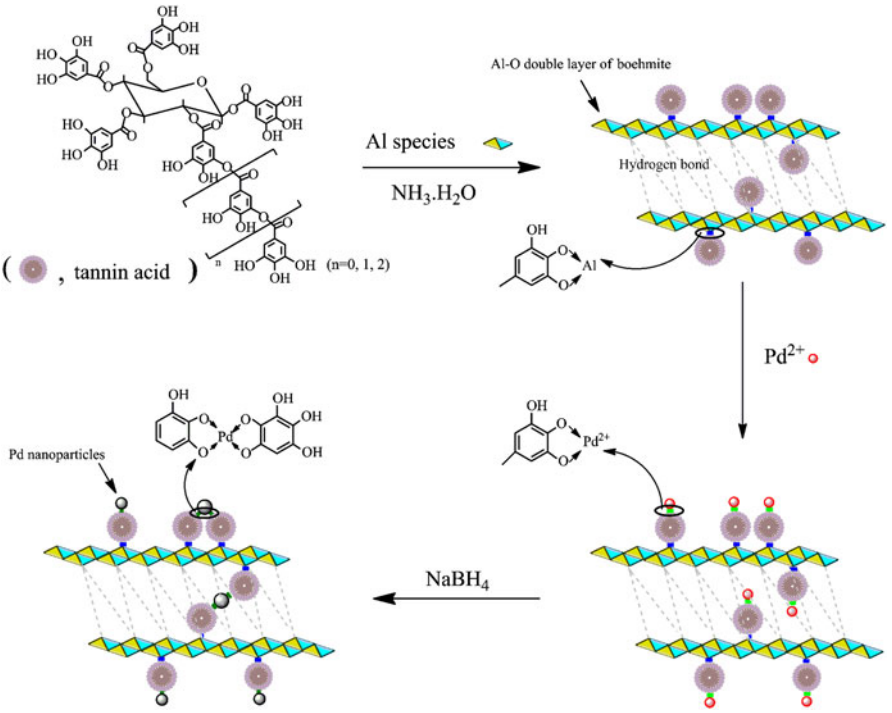

Fig. 2 Schematic illustration showing the general synthetic procedures of Pd–TA–boehmite

Effect of tannic acid

The introduction of tannic acid influences the crystallization of boehmite. As shown in Fig. 3, the diffraction patterns of the as-prepared samples exhibit the features of boehmite (JCPDS #21-1307). However, the diffraction peaks of Pd–TA–boehmite are boarder and less intense, which indicates that Pd–TA–boehmite had lower crystallinity and/or smaller crystallites. Possibly, the chelation interaction between phenolic hydroxyls of tannic acid and Al^{3+} species increased the nucleus number of boehmite crystallites, which inhibited the normal growth process of boehmite crystallites. Further observation reveals that the XRD pattern of Pd–boehmite shows the (111) refection of Pd(0) crystal at $2\theta = 40.2^{\circ}$, while no peaks related to Pd species can be observed in the XRD pattern of Pd–TA–boehmite because of weak intensity of total XRD patterns of the Pd–TA–boehmite catalyst. These differences in XRD patterns may mean that small Pd(0) nanoparticles with good dispersion were formed in the Pd–TA–boehmite catalyst, which is confirmed by following TEM observations.

The influence of tannic acid on the textural properties of boehmite was investigated by N_2 adsorption/desorption method. As shown in Fig. 4, the specific

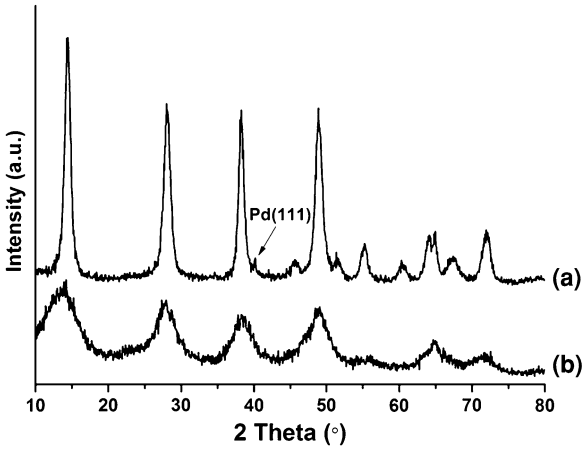

Fig. 3 XRD patterns of the as-prepared Pd–boehmite (**a**) and Pd–TA–boehmite (**b**)

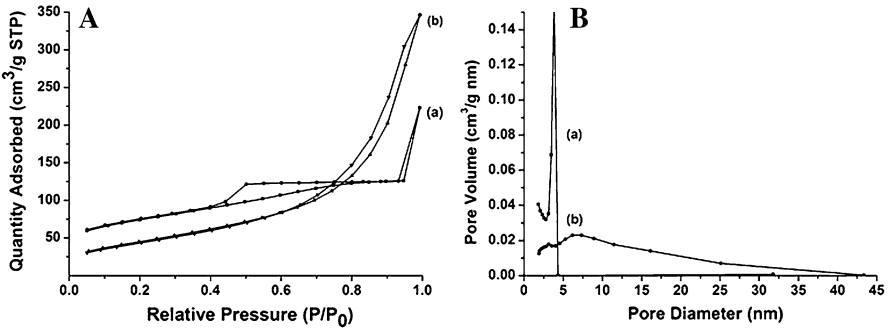

Fig. 4 N_2 adsorption–desorption isotherms (A) and pore size distribution (B) of Pd–TA–boehmite (**a**) and Pd–boehmite (**b**)

surface area of the Pd–TA–boehmite catalyst is determined to be about 268.65 m^2 g^{-1}, much higher than that of Pd–boehmite (168.14 m^2 g^{-1}). It is generally accepted that the catalysts with high surface area provide more active sites and enable more chemicals to participate in reactions [26]. Compared with the Pd–boehmite catalyst, the Pd–TA–boehmite catalyst shows much narrower pore distribution. Thus, it is reasonable to believe that the obtained Pd–TA–boehmite should have higher activity and selectivity in catalytic reactions. Considering that all the other experimental parameters are similar, the changes in textural structure of the catalyst should be caused by tannic acid, which directed the crystal growth of boehmite via the interaction between tannic acid and the growing boehmite crystal. Further work is underway to study the underlying mechanisms.

TEM observations show substantial differences in particle size and dispersion of the Pd nanoparticles contained in the Pd–TA–boehmite catalyst and in the Pd–boehmite catalyst. As shown in Fig. 5A, the Pd nanoparticles with the small size

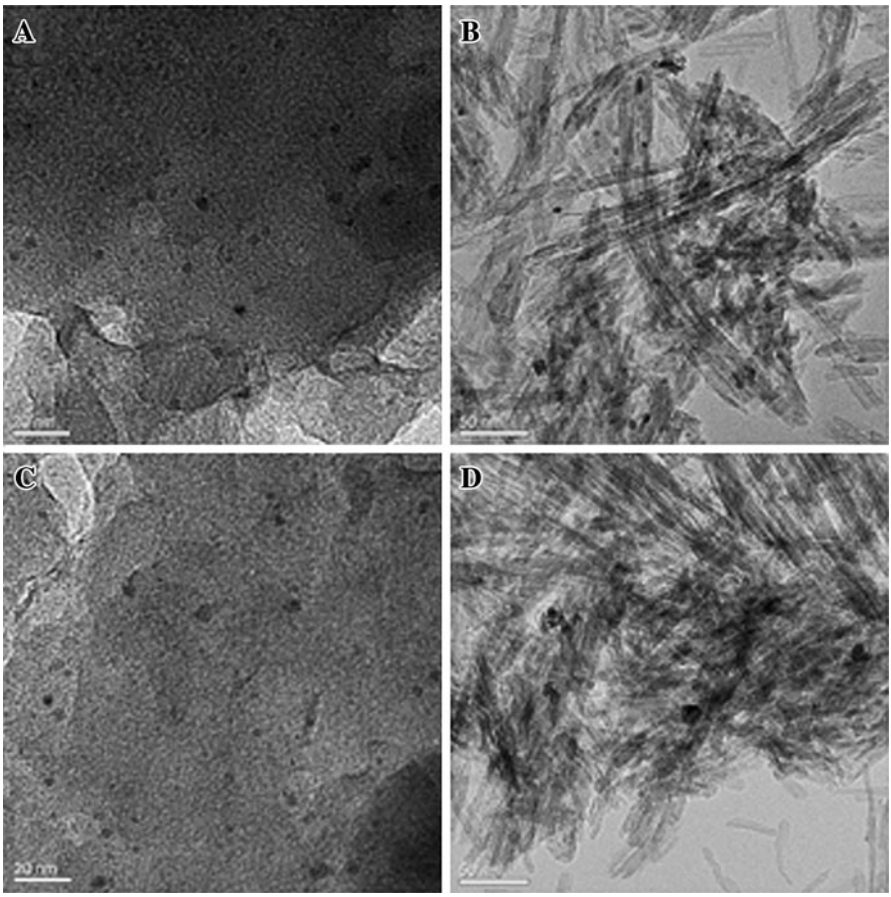

Fig. 5 TEM images of Pd–TA–boehmite (**A**), Pd–boehmite (**B**), Pd–TA–boehmite after seven cycles in hydrogenation reaction (**C**) and Pd–boehmite after four cycles in hydrogenation reaction (**D**)

of 3.6 nm are highly dispersed in the Pd–TA–boehmite catalyst. In contrast, the Pd nanoparticles in the Pd–boehmite catalyst (Fig. 5B) show poor distribution, and have the relatively larger size of 8.5 nm. Occasionally, some Pd nanoparticles are larger than 15 nm, indicating that the Pd nanoparticles suffered serious aggregation in the Pd–boehmite catalyst. These results are consistent with the XRD analysis. As for the Pd–TA–boehmite catalyst, tannic acid could serve as an effective stabilizer to suppress the excessive growth and aggregation of the Pd nanoparticles, which ensured the small size and good dispersion of the Pd nanoparticles. However, in the absence of tannic acid, Pd nanoparticles would be overgrowth and/or aggregations on boehmite.

Catalytic activity evaluation

Table 1 shows the catalytic results of the as-prepared catalysts in the hydrogenation of olefins with different structures. For all substrates, the Pd–TA–boehmite catalyst was found to be more active than the Pd–boehmite catalyst. Especially in the hydrogenation of ally alcohol, the initial hydrogenation rate and selectivity of the Pd–TA–boehmite catalyst reached 23,520 mol/mol h and 99 %, respectively, much higher than those of the Pd–boehmite catalyst (14,186 mol/mol h and 93 %). The obvious improvements of catalytic activity and selectivity of the Pd–TA–boehmite catalyst are the contribution of tannic acid to the distribution of Pd nanoparticles and the textural properties of the boehmite. As confirmed by TEM and N_2 absorption/desorption determinations, compared with Pd–boehmite, Pd–TA–boehmite has a higher specific surface area and well-distributed Pd nanoparticles of much smaller size, which provides a larger fraction of exposed active Pd atoms available for more substrates to participate in reactions, thus leading to higher catalytic activity. On the other hand, the narrower pore distribution of the Pd–TA–boehmite catalyst is beneficial for the molecular-shape selectivity of the reaction and efficiently inhibits

Table 1 Catalytic activity and selectivity of the catalysts for the hydrogenation of olefins

Catalyst	Substrate	Initial hydrogenation rate (mol mol h^{-1})	Selectivity (%)	Conversion (%)
Pd–TA–boehmite	Allyl alcohol	23,520	>99[a]	89.3
Pd–TA–boehmite	a-Methacrylic acid	17,600	100[b]	73.2
Pd–TA–boehmite	Styrene	13,920	100[c]	58.1
Pd–boehmite	Allyl alcohol	14,186	93[a]	59.2
Pd–boehmite	a-Methacrylic acid	12,750	100[b]	53.4
Pd–boehmite	Styrene	11,230	100[c]	49.2

Catalyst/substrate 2.5 μmol/10 mmol, solvent 20.0 mL methanol, temperature 30 °C, H_2 pressure 1.0 MPa, Stirring rate 1,200 rpm, Reaction time 10 min

[a] The selectivity to propanol

[b] The selectivity to isobutyricacid

[c] The selectivity to phenylethane

side reactions of isomerization. Meanwhile, it is noted that the catalytic activity advantage of the Pd–TA–boehmite catalyst over the Pd–boehmite catalyst was reduced but still evident when the substrates with side chain (a-methacrylic acid) or large molecules (styrene) were used. As shown in Table 1, the initial hydrogenation rate of allyl alcohol on the Pd–boehmite catalyst was 14,186 mol/mol h, and it was increased to 23,520 mol/mol h on the Pd–TA–boehmite catalyst, an increase of 65.8 %. However, when a-methacrylic acid and styrene were used as the substrates, the initial hydrogenation rates were increased by 38.0 and 24.0 %, respectively. The reasons for these differences should mainly be ascribed to the steric hindrance of substrates with side chain or large molecules making it difficult for the substrates to access the Pd nanoparticles located in the porosity of the Pd–TA–boehmite catalyst.

Heterogeneous metal nanocatalysts often suffer the problems of leaching and aggregation of active species during their recycling and eventually lose their catalytic activity [6, 7]. In the present investigation, however, the Pd–TA–boehmite catalyst exhibited much higher stability during its recycling use. As shown in Fig. 6, the catalytic activity of the Pd–TA–boehmite catalyst was hardly reduced when recycled in the hydrogenation of allyl alcohol, and its hydrogenation rate was still as high as 20,791 mol/mol h at the 7th repeated application. According to the analysis of ICP-AES, the loss of Pd amount was determined to be only 8.3 %, and no obvious aggregation of the Pd nanoparticles was observed in the TEM image (Fig. 5C). In contrast, the Pd–boehmite catalyst suffered a sharp decrease in catalytic activity after four cycles, of which the hydrogenation rate reduced to 5,250 mol/mol h, only retaining 37 % of its initial activity. Based on the ICP-AES analysis, the loss of Pd content in the Pd–boehmite catalyst was 56 % after recycled four times, and serious aggregation of Pd nanoparticles was also observed (Fig. 5D). These results confirm that tannic acid plays a crucial role in achieving high reusability for the Pd–TA–boehmite catalyst, which ensures the stability and even dispersion of Pd nanoparticles.

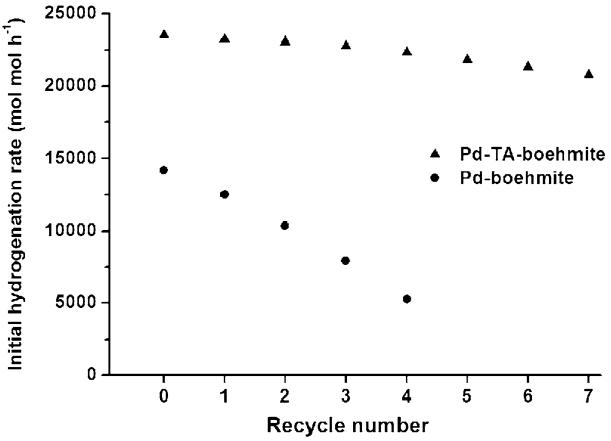

Fig. 6 Recycles of Pd–TA–boehmite and Pd–boehmite in the hydrogenation of allyl alcohol

Conclusions

In this work, we prepared a highly active and reusable Pd catalyst (Pd–TA–boehmite) by a hydrothermal method using tannic acid as the structure-directing agent as well as stabilizer. The use of tannic acid increased the specific surface area of the boehmite, and narrowed the pore distribution, which was beneficial for the high activity of the Pd–TA–boehmite catalyst. Moreover, tannic acid can act as a stabilizer to link Pd nanoparticles and boehmite, which ensured the high stability of the Pd–TA–boehmite catalyst during recycles. In addition, this strategy might be applied to the synthesis of other high-performance metal nanoparticle catalysts considering that tannic acid has the ability to chelate with many kinds of metal ions.

Acknowledgments We acknowledge the financial supports provided by the National Natural Science Foundation of China (21,176,161) and National High Technology R&D Program (2011AA06A108). We also give thanks to Test Center of Sichuan University for the help of TEM tests.

References

1. C.N. Ramachandra Rao, G.U. Kulkarni, P.J. Thomas, P.P. Edwards, Chem. Soc. Rev. **29**, 27 (2000)
2. Y. Xia, Y. Xiong, B. Lim, S.E. Skrabalak, Angew. Chem. Int. Ed. **48**, 60 (2008)
3. A.R. Tao, S. Habas, P. Yang, Small **4**, 310 (2008)
4. S. Che, Z. Liu, T. Ohsuna, K. Sakamoto, O. Terasaki, T. Tatsumi, Nature **429**, 281 (2004)
5. R. Chauhan, A. Kumar, R.P. Chaudhary, Res. Chem. Intermed. **38**, 1443 (2012)
6. A. Kumar, S. Mandal, P.R. Selvakannan, R. Pasricha, A.B. Mandale, M. Sastry, Langmuir **19**, 6277 (2003)
7. J.S. Zheng, X.S. Zhang, P. Li, J. Zhu, X.G. Zhou, W.K. Yuan, Electrochem. Commun. **9**, 895 (2007)
8. Y.R. Uhm, H.M. Lee, F. Olga, O. Irina, V. Marina, R. Gennady, C. Valery, C.K. Rhee, Res. Chem. Intermed. **36**, 867 (2010)
9. J. Zhu, Z. Konya, V.F. Puntes, I. Kiricsi, C.X. Miao, J.W. Ager, A.P. Alivisatos, G.A. Somorjai, Langmuir **19**, 4396 (2003)
10. J.S. Chang, J.S. Hwang, S.E. Park, Res. Chem. Intermed. **29**, 921 (2003)
11. E. Ruckenstein, Z.F. Li, Adv. Colloid Interface Sci. **113**, 43 (2005)
12. L.C. de Santa Maria, A.L.C. Santos, P.C. Oliveira, H.S. Barud, Y. Messaddeq, S.J.L. Ribeiro, Res. Chem. Intermed. **63**, 797 (2009)
13. J.H. He, T. Kunitake, A. Nakao, Chem. Mater. **15**, 4401 (2003)
14. Y. Zhou, W.X. Chen, H. Itoh, K. Naka, Q.Q. Ni, H. Yamane, Y. Chujo, Chem. Commun. **23**, 2518 (2001)
15. X. Huang, H. Mao, X.P. Liao, B. Shi, Catal. Commun. **12**, 1000 (2011)
16. H. Wu, X. Huang, M.M. Gao, X.P. Liao, B. Shi, Green Chem. **13**, 651 (2011)
17. T.B. He, L. Xiang, S.L. Zhu, Langmuir **24**, 8284 (2008)
18. H.Y. Zhu, J.D. Riches, J.C. Barry, Chem. Mater. **14**, 2086 (2002)
19. Y. Mathieu, B. Lebeau, V. Valtchev, Langmuir **23**, 9435 (2007)
20. G. Vázquez, J. González-Álvarez, F. López-Suevos, G. Antorrena, Bioresour. Technol. **87**, 349 (2003)
21. P. Kacer, L. Late, M. Kuzma, L. Cerveny, J. Mol. Catal. A. **159**, 365 (2000)
22. J.A. Rotole, P.M.A. Sherwood, Surf. Sci. Spectra **5**, 53 (1998)
23. R. Flamia, G. Lanza, A.M. Salvi, J.E. Castle, A.M. Tamburro, Biomacromolecules **6**, 1299 (2005)
24. R. Lapuente, C. Quijada, F. Huerta, F. Cases, J.L. Vazquez, Polym. J. **35**, 911 (2003)
25. C. Evangelisti, N. Panziera, P. Pertici, G. Vitulli, P. Salvadori, C. Battocchio, G. Polzonetti, J. Catal. **10**, 287 (2009)
26. X. Bokhimi, J.A. Toledo-Antonio, M.L. Guzmán-Castillo, F. Hernández-Beltrán, J. Solid State Chem. **161**, 319 (2001)